EXPERIMENTAL MEASUREMENT OF THE DRAG COEFFICIENT*

T. Vreeland, Jr., and K.M. Jassby
W.M. Keck Laboratory of Engineering Materials
California Institute of Technology
Pasadena, California 91109

The drag coefficient is related to the dissipative viscous force which acts on a dislocation in motion. The magnitude of the drag coefficient for a dislocation of known Burgers vector is determined by measurement of the viscous force at known dislocation velocity, or by measurement of the energy dissipation brought about by the viscous force. We discuss here these measurements and explore the special conditions which make possible the determination of the drag coefficient.

DISSIPATIVE AND NON-DISSIPATIVE FORCES

When the dissipative viscous drag force predominates over all other forces which retard dislocation motion, a constant resolved shear stress, τ, will produce a terminal dislocation velocity, v, such that the driving force per unit dislocation length, τb, is equal to the viscous force per unit length, Bv, where B is the drag coefficient and b is the Burgers vector. Thus

$$B = \frac{\tau b}{v} \quad . \tag{1}$$

The most direct determination of B is the measurement of v for a

*This work was supported by the U. S. Atomic Energy Commission and the California Institute of Technology.

known τ and b under conditions where eq. 1 applies. This approach is complicated by the existence of non-dissipative forces which also act on the moving dislocation. Interactions between the moving dislocation and nearby surfaces, other dislocations, and point defects all give rise to non-dissipative forces, as do Peierls forces, inertial forces and curvature forces. These forces will usually vary as the dislocation moves through the crystal and the variation may have a characteristic wave length, λ. It is then useful to consider the mean dislocation velocity, $\bar{v}$, over a distance large compared to λ. In many cases the non-dissipative forces will have the effect of reducing the driving force on the dislocation. Then $\bar{v}$ will be less than the terminal velocity, v, that would be attained for the same applied resolved stress in the absence of non-dissipative forces. In one important case, i.e., the growth of slip bands, the forces on the leading dislocation due to those following may make $\bar{v}$ larger than v.

A linear, or viscous, relationship between $\bar{v}$ and the applied resolved stress may result from the influence of drag mechanisms which are non-dissipative. For example, $\bar{v}$ vs. τ measurements in the diamond cubic lattice[1] have shown a linear relationship to be followed. Thermal activation over the Peierls barrier, a non-dissipative process, is thought to be responsible for determining the linear $\bar{v}$ vs. τ relationship. Viscous drag forces also act in this case, but they do not directly influence the $\bar{v}$ vs. τ relationship and the drag coefficient cannot be obtained from this data. The direct determination of B using eq. 1 requires that the non-dissipative forces be small compared to the dissipative force (or that they be

accurately known and taken into account). The non-dissipative forces do not similarly complicate the determination of B from measurements of energy dissipation (i. e. the internal friction method).

THE DIRECT METHOD

A calculation of the stresses and velocities involved in direct measurements of B is useful to show the importance of accounting for non-dissipative forces. Drag coefficients of the order or 10^{-4} cgs are typical. Taking $b = 2.5 \times 10^{-8}$ cm, eq. 1 gives $v = 250$ cm/sec/bar. We see immediately that we must be prepared to either measure high dislocation velocities or conduct the experiments at very low stresses. The flow stress of the crystal is a fair measure of the effective non-dissipative stresses, and as discussed above, the applied stress must be greater than these stresses for the direct method to apply. For this reason the applied resolved shear stress in the direct method will usually be greater than one bar. High dislocation velocities are therefore necessary, and continuous observation of high velocity dislocations is not currently possible. The stress pulse technique, in which mean velocities are deduced from dislocation displacement observations is the most direct method available.

Stress pulse techniques have been reviewed elsewhere.[2] The stress pulse must be of short enough duration to stop the dislocations before they move out of the crystal. Longitudinal and torsional stress pulses in rods have been used for measurement of the drag coefficient. As the high velocity dislocations are not

continuously observed, the entire stress-time history between dislocation observations must be known. Careful attention must therefore be given to possible wave reflections which could cause multiple stress pulses in the specimen.

An example of the use of a torsional stress pulse and Berg-Barrett topography for dislocation displacement measurements is shown in fig. 1. The topograph of an (0001) surface of zinc in fig. 1a was taken after scratching the surface to introduce basal edge dislocations. Kodak-type R X-ray film was used with an exposure time of 12 min. A higher resolution film or plate would require a longer exposure and therefore a longer time between the introduction of the dislocations and the application of a stress pulse. This time is held to a minimum in the experiments to minimize climb and impurity pinning of the fresh dislocations. Figure 1b shows a topograph taken after a torsional stress pulse was applied to the (0001) end surface of the cylindrical crystal. This topograph was made using a Kodak high-resolution plate and required a 9 hour exposure. The stress pulse caused the dislocation displacements which are seen to vary linearly with radius. The applied resolved shear stress amplitude varied linearly with radius, and a knowledge of the torsional pulse amplitude and the duration permits us to relate the displacements of fig. 1b to dislocation velocity and the radial position to stress amplitude (maximum values in fig. 1b were 6.6×10^3 cm/sec and 25 bar). The leading dislocation line of fig. 1b then represents the velocity vs. stress curve. The slope of this curve, together with a knowledge of b (whose direction is confirmed by topographs using $\{10\bar{1}3\}$ reflections for which $\bar{g} \cdot \bar{b} = 0$) gives B using eq. 1. A linear velocity-

stress relationship is observed in fig. 1b at stress levels as low as one bar, which indicates that non-dissipative forces were either very small or were linearly dependent on $\bar{v}$. The temperature dependence of B determined in these experiments[3] is the opposite of that expected when the $\bar{v}$ vs. τ curve is controlled by thermally activated processes. This observation, and the agreement between the B values determined in the direct experiments and in the internal friction experiments leads us to believe that we have succeeded in making the non-dissipative forces negligible compared to the Bv forces.

When a crystal is hardened by discrete obstacles, the drag coefficient may be found from $\bar{v}$ vs. τ measurements at stresses larger than about twice the critical resolved stress. Figure 2 shows an example of this in zinc where the discrete obstacles were forest dislocations introduced by second-order pyramidal slip. The critical stress to move basal dislocations through the forest with a dislocation density of 7×10^4 /cm^2 is about 3 bar, and at stresses of about 6 bar the $\bar{v}$ - τ relationship becomes linear (extrapolating to the origin) with the same slope found in crystals with a much lower forest density (and a critical stress less than 1 bar). This behavior, with a transition from obstacle controlled velocity to viscous drag controlled velocity with increasing stress was predicted by Frost and Ashby.[5] A similar transition has been observed in the $\bar{v}$ - τ relations for screw dislocations on the second-order pyramidal slip planes of zinc.[6] At resolved stress levels below about 20 bar, Lavrentev et. al. found the $\bar{v}$ vs. τ curve to be non-

linear, and the stress at the transition is likely to be a Peierls stress. We have recently confirmed this transition for both screw and edge oriented dislocations on the second-order pyramidal system of zinc using longitudinal stress waves which produce a single short duration stress pulse in the crystal. Dislocations are observed after the pulse is applied using Berg-Barrett X-ray topography. Individual dislocations in a slip band are resolved in the topograph shown in fig. 3. The dislocation interaction forces may be calculated knowing the dislocation positions, so that an estimate of their importance compared to the viscous force may be made.

Attempts have been made to obtain the drag coefficient from measurement of the strain rate vs. stress relation at strain rates above about 10^2/sec. The product of mobile dislocation density and the average dislocation velocity may be related to the strain rate. Hence, a knowledge of the mobile dislocation density is needed to determine the average dislocation velocity. Only an estimate of the mobile dislocation density can be made, since it cannot be measured under the test conditions. Therefore, reliable estimates of the dislocation velocities in these tests cannot be made. Nagata and Yoshida[7] estimated that the mobile dislocation density at plastic strain rates between 7×10^2/sec and 2×10^3/sec was equal to the initial density determined from etch pit counts ($\rho = 5 \times 10^6/cm^2$), and calculated $B = 2.4 \times 10^{-4}$ from the slope of the linear strain rate vs. τ relationship they found at small plastic strains in copper at room temperature. We have determined a value of $B = 2.0 \times 10^{-4}$ for copper from torsional stress pulse tests at room temperature.

INTERNAL FRICTION MEASUREMENTS

Dislocations are assumed to be strongly pinned by a network of discrete obstacles (usually dislocation nodes) and more weakly pinned at intermediate locations by point defects in the Granato-Lücke theory[8] which described dislocation-induced energy loss mechanisms in internal friction experiments. Each dislocation, excited by an externally applied oscillating stress field, vibrates between its pinning points. Two distinct cases have been considered: (i) during each cycle of stress, the dislocation breaks away from the weaker pinning points, but remains pinned at its network lengths, and (ii) the dislocation remains pinned at each discrete obstacle throughout the stress oscillation. In the former case, called amplitude-dependent internal friction, (see also Ref. 9) dislocation damping is derived from both hysteretic effects attributed to dislocation breakaway from intermediate pinning points and phase lag effects induced by linear or viscous damping. The energy loss (decrement) is a function of the amplitude of the exciting stress. In the latter or amplitude independent case, (see also Ref. 10) only phase lag losses are considered, and the decrement is a function of the oscillating frequency of the applied stress.

In both experimental situations, dislocation-induced losses can be separated from those losses attributed to direct interaction between the exciting stress wave and the crystal by carrying out the experimental measurements both before and after neutron irradiation of the crystal.[11] The strong pinning of dislocations by irradiation induced defects should make the dislocation induced losses negligible

compared to the other losses. Highly perfect crystals are not employed for these experiments because they do not contain a sufficient density of mobile dislocation line to induce a measurable decrement. Both cases demand low resolved shear stresses and consequently small dislocation velocities (of the order of 10cm/sec).

In the most simple dislocation model, edge and screw dislocations are not treated separately, but rather "averaged" values are implied for the various parameters which enter the theory. Granato and Stern[12] have shown that when dislocations of more than one orientation contribute to energy absorption, a much broader peak in the curve for decrement as a function of exciting frequency results than in the situation where only one type of dislocation is active. In the former case, accurate analysis of experimental measurements precludes treatment on the basis of the simpler model. In one internal friction experiment in copper,[12] where a broad peak was observed in the decrement vs. frequency curve, the measurements were analyzed by considering contributions from both edge and screw oriented dislocations. In this case the magnitude of B deduced was in good agreement with that derived from direct measurements.[13]

The energy loss from a network of vibrating dislocations is normally characterized by two geometric parameters, the average dislocation loop length and the total length of mobile dislocation line, values of which must be estimated for each particular crystal in order to interpret the decrement measurements and hence evaluate B. Under certain experimental conditions the decrement is independent of the average loop length.[11] Two experimental techniques

have recently been developed which enable one to determine B independently of knowledge of these two parameters. The first technique[14] applies to the measurement of B below the superconducting transition temperature in superconducting metals.* The second technique,[15] which employs a bias stress, is applicable to all materials over an extended temperature range. Both methods provide more promising solutions to the problem of measuring B at low dislocation velocities, by removing the uncertainties inherent in estimation of the average dislocation loop length and the total length of mobile dislocation line. However, B cannot be deduced independently of the dislocation effective mass with these techniques. This latter quantity must be estimated from theoretical considerations and the value of B will depend on the accuracy of this estimation.

*Hikata and Elbaum, discussing this method, assumed that conduction electrons provide the only significant source of dislocation damping at temperatures near absolute zero and hence the value of B in the superconducting state is negligible compared to that in the normal state. Recent experimental work carried out by the present authors has indicated the presence of a residual phonon damping in copper at 4.2°K, contrary to this assumption.

FIGURE CAPTIONS

Fig. 1. Berg-Barrett topographs of an (0001) end surface of a zinc cylinder, $(10\bar{1}3)$ reflection, $CoK\alpha$, 40 Kv, 7 ma, 26.5 X. Center of cylinder is at the left edge of the topograph. a) After scratching, b) After application of a torsional stress pulse at $66^{o}K$.

Fig. 2. Berg-Barrett topograph of an (0001) surface of zinc containing a forest dislocation density of about $7 \times 10^{4}/cm^{2}$, after scratching and applying a torsional stress pulse, $(10\bar{1}3)$ reflection, 40X.

Fig. 3. Berg-Barrett topograph of an (0001) surface of zinc after application of a 7 μsec duration compression stress pulse along $[1\bar{2}10]$, $(10\bar{1}3)$ reflection, 135X.

REFERENCES

1. S. Schafer, Phys. Status Solidi, 19, 297 (1967).
2. T. Vreeland, Jr., Techniques of Metals Research, Volume II, Part 1, R.F. Bunshah, ed., Interscience Publishers, 1968, p. 341.
3. T. Vreeland, Jr., and K.M. Jassby, Mat. Sci. Eng. 7, 95 (1971).
4. N. Nagata and T. Vreeland, Jr., Phil. Mag. 25, 1137 (1972).
5. H.J. Frost and M.F. Ashby, J. Appl. Phys. 42, 5273 (1971).
6. F.F. Lavrentev, O.P. Salita, and V.L. Vladimirova, Phys. Stat. Sol. 29, 569 (1968).
7. N. Nagata and S. Yoshida, J. Met. Soc. Japan 32, 385 (1968).
8. A. Granato and K. Lücke, J. Appl. Phys. 27, 583 (1956).
9. D.H. Rogers, J. Appl. Phys., 33, 781 (1962).
10. A. Granato, in Dislocation Dynamics, McGraw-Hill, New York, 1968, p. 117.
11. G.A. Alers and K. Salama, in Dislocation Dynamics, McGraw-Hill, New York, 1968, p. 211.
12. R.M. Stern and A.V. Granato, Acta Met. 10, 358 (1962).
13. K.M. Jassby and T. Vreeland, Jr., Phil. Mag. 21, 1147 (1970).
14. A. Hikata and C. Elbaum, Trans. Jap. Inst. Met. Suppl. 9. 46 (1968).
15. A. Hikata, R.A. Johnson, and C. Elbaum, Phys. Rev. 2, 4856 (1970).

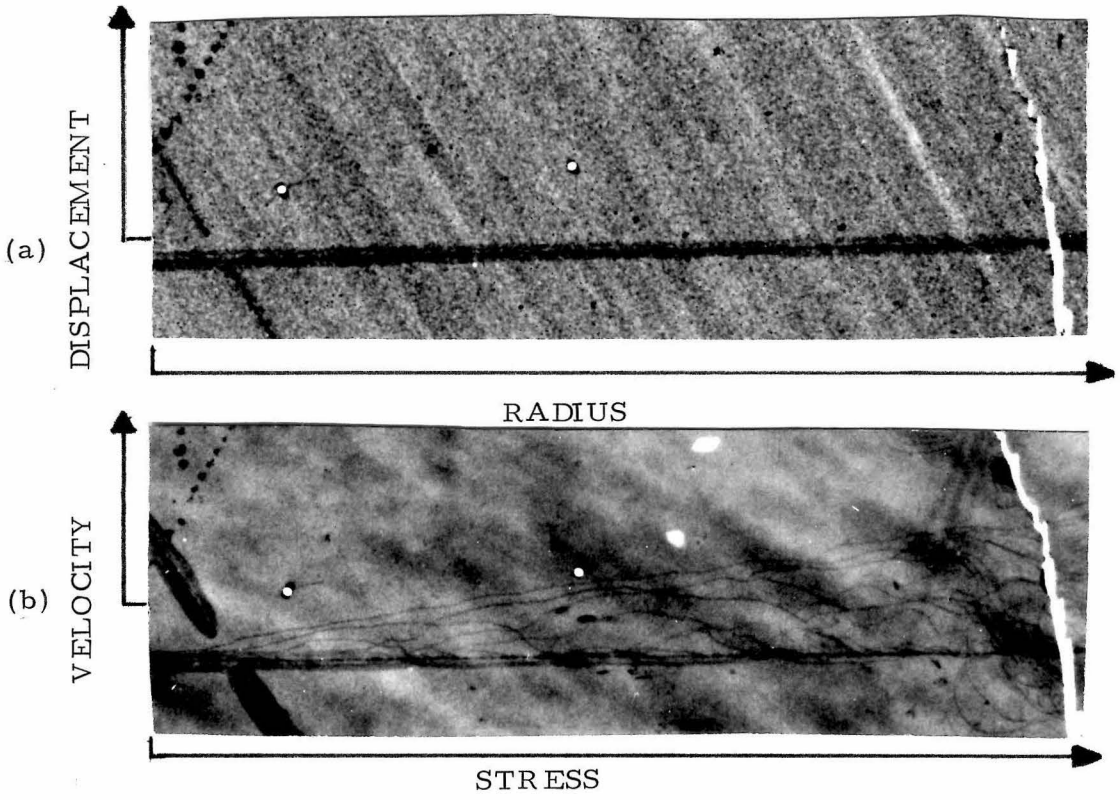

Fig. 1. Berg-Barrett topographs of an (0001) end surface of a zinc cylinder, $(10\bar{1}3)$ reflection, CoKα, 40 Kv, 7 ma, 26.5 X. Center of cylinder is at the left edge of the topograph. a) After scratching, b) After application of a torsional stress pulse at 66^{o}K.

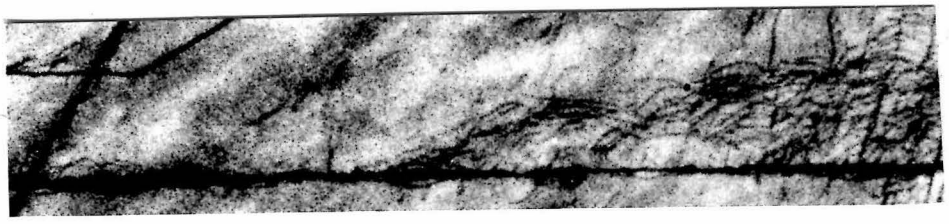

Fig. 2. Berg-Barrett topograph of an (0001) surface of zinc containing a forest dislocation density of about $7 \times 10^{4}/cm^{2}$, after scratching and applying a torsional stress pulse, $(10\bar{1}3)$ reflection, 40 X.

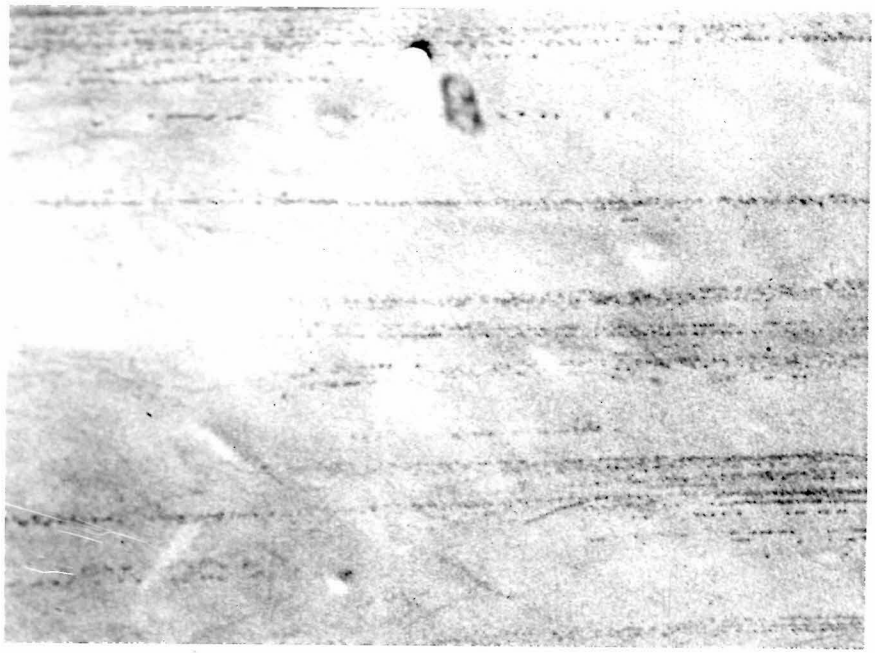

Fig. 3. Berg-Barrett topograph of an (0001) surface of zinc after application of a 7 μsec duration compression stress pulse along $[12\bar{1}0]$, $(10\bar{1}3)$ reflection, 135 X.